Journal of Engineering Science, Vol. 16(2), 101–110, 2020

Effect of Carbonate to Phosphate Molar Ratios on the Physico-Chemical Properties of Carbonated Hydroxyapatite Nanopowder

Muhammad Syazwan Mohd Noor, Nur Nabilah Afja Mohd Afandi, Ahmad-Fauzi Mohd Noor and Yanny Marliana Baba Ismail*

Biomaterials Niche Group, School of Materials and Mineral Resources Engineering, Engineering Campus, Universiti Sains Malaysia, 14300 Nibong Tebal, Pulau Pinang, Malaysia

*Corresponding author: yannymarliana@usm.my

Published online: 10 December 2020
To cite this article: Muhammad Syazwan Mohd Noor, Nur Nabilah Afja Mohd Afandi, Ahmad-Fauzi Mohd Noor and Yanny Marliana Baba Ismail (2020). Effect of carbonate to phosphate molar ratios on the physico-chemical properties of carbonated hydroxyapatite nanopowder. *Journal of Engineering Science*, 16(2), 101–110, https://doi.org/10.21315/jes2020.16.2.5.
To link to this article: https://doi.org/10.21315/jes2020.16.2.5

Abstract: *The aim of this study was to incorporate carbonate ions (CO_3^{2-}) into the hydroxyapatite (HA) crystal structure followed by investigation on the effect of different carbonate to phosphate (CO_3^{2-}/PO_4^{3-}) ratios on the phase purity, crystal structure as well as CO_3^{2-} content present in the apatite structure. CO_3^{2-} substitution has been proposed to enhance the performance of HA-based material, particularly on the physico-chemical properties. Three different compositions of carbonated hydroxyapatite (CHA) powder with different CO_3^{2-}/PO_4^{3-} ratios (namely, CHA 1:1, CHA 2:1 and CHA 4:1) were chemically synthesised by nanoemulsion method at 37°C and characterised for their physico-chemical properties. Results demonstrated that all as-synthesised powders formed single phase B-type CHA without any additional phases. Interestingly, an increasing amount of CO_3^{2-} substituted into the apatite structure gives rise to the formation of CHA structure with a variation on their cell parameters and the degree of crystallinity. An increase in the CO_3^{2-}/PO_4^{3-} ratio was also found to lead a higher amount of CO_3^{2-} content present in the as-synthesised powder (in a range of 4 wt % to 10 wt %), which is comparable to the CO_3^{2-} content found in the human bone mineral.*

Keywords: carbonate to phosphate ratio, carbonated hydroxyapatite, nanoemulsion

1. INTRODUCTION

Hydroxyapatite (HA), $Ca_{10}(PO_4)_6(OH)_2$ is one of the calcium-phosphate-based materials, which had been widely used as bone and dental materials due to its affinity to the mineralised phase of natural human bone and tooth. HA also demonstrated to have a good biocompatibility, bioactivity and osteoconductivity properties.[1,2] Despite its advantages, HA has been reported to have significant drawbacks, where its resorption *in vivo* is too sluggish to induce the formation of new bone tissue and in terms of composition, HA is lacking of minor trace elements found in native bone, i.e. carbonate (CO_3^{2-}), orthosilicate (SiO_4^{4-}), magnesium ion (Mg^{2+}), cobalt ion (Co^{2+}), strontium ion (Sr^{2+}) and zinc ion (Zn^{2+}).[3] Besides, HA is also known to possess low mechanical properties, due to its brittleness, rigid, lack of strength and low wear resistance which limits its application for load-bearing applications.[1,4]

In recent years, researchers worldwide have been realised that the mineral phase of human bone is not solely calcium phosphate, but also composed of a number of ions, where CO_3^{2-} is the most abundant species (2 wt % to 10 wt %) found in native bone.[5,6] The incorporation of CO_3^{2-} ions in HA was reported to increase the dissolution rate and solubility, which directly enhances its osteointegration rate.[7] Thus, carbonated hydroxyapatite (CHA) seems like a promising bone material since its chemical composition is more akin to the main inorganic mineralised part of the native bone mineral as compared to stoichiometric HA.[8,9]

The classification of CHA usually depends on the mode of CO_3^{2-} substitution in the apatite structure, either the CO_3^{2-} ions substituted into hydroxyl (OH^-) or phosphate (PO_4^{3-}) sites forming A- or B-type CHA, respectively.[10] According to literature, B-type CHA is the preferable CO_3^{2-} substitution, which commonly found in young native bone with the ratio of A/B in the range of 0.7 and 0.9.[11] The ratio varies depending on the individual's age. For instance, a higher A/B ratio was observed in old bone tissue and this is referred as A-type CHA, whereas B-type CHA is typically found in young bone tissue.[12] Various synthesis routes used to produce CHA-based materials, including hydrothermal, sol-gel, precipitation, mechano-chemical, mechanical activation and nanoemulsion method.[13] Among these methods, nanoemulsion is one of the promising methods in synthesising B-type CHA nanopowder with low crystallinity.[14] Besides that, this method is commonly selected because of its simple process, availability of the equipment and also simply adjustable parameters with potentially good yields.[15]

Therefore, the present work aims to study the effect of varying carbonate to phosphate (CO_3^{2-}/PO_4^{3-}) molar ratios on the physico-chemical properties of CHA powder. Several characterisation techniques were applied to analyse the produced powders such as X-ray diffraction (XRD) analysis, carbon, hydrogen and nitrogen (CHN) analysis, Fourier transform infrared (FTIR) spectroscopy and field emission scanning electron microscopy (FESEM) equipped with energy dispersive X-ray (EDX) analysis.

2. MATERIALS AND METHODS

2.1 Powders Synthesis

CHA powder with three different CO_3^{2-}/PO_4^{3-} ratios (namely, CHA 1:1, CHA 2:1 and CHA 4:1) were produced by direct pouring nanoemulsion method. High grade purity of starting materials comprising di-ammonium hydrogen phosphate ($(NH_4)_2HPO_4$), calcium nitrate tetrahydrate ($Ca(NO_3)_2.4H_2O$) and ammonium bicarbonate ($(NH_4)HCO_3$) were used in this study. To prepare CHA 1:1, two aqueous solutions of $(NH_4)_2HPO_4$ and $(NH_4)HCO_3$ were firstly prepared separately by dissolving in 60 mL deionised water. The calcium source ($Ca(NO_3)_2.4H_2O$) was then prepared by dissolving in 100 mL acetone and directly poured into the previously mixed solution. The mixture was continuously stirred for 60 min to obtain a homogenous mixture. The pH of the mixture was carefully adjusted to pH 11 by adding 1 M sodium hydroxide (NaOH). Milky-waxy white mixture was subsequently filtered and washed with deionised water three times to remove any residues. The filtered cake was dried in the oven at 90°C for 24 h. Lastly, the dried cake was then crushed and sieved (using 90 μm siever) prior to physico-chemical characterisations. Similar preparatory procedure was carried out for CHA 2:1 and CHA 4:1 by changing the amount of CO_3^{2-}.

2.2 Characterisation Techniques

The phase formation and crystallinity of the as-synthesised CHA powders with different CO_3^{2-}/PO_4^{3-} ratios produced were identified by XRD (Bruker D8 XRD) with a copper anode (Cu Kα, λ = 1.5406 Å) as X-ray source. The reflection patterns were fixed from 2-Theta, 2 θ = 20° to 70° with a step size of 0.02°. Phase determinations were made accordance to reference pattern of stoichiometric HA (ICDD [International Centre for Diffraction Data] file no. #09-0432). The mode of CO_3^{2-} substitution (i.e., A- or B-type CHA) within the apatite structure was confirmed by FTIR spectroscopy. The FTIR spectra were scanned four times at wavelength intervals from 400 cm^{-1} to 4,000 cm^{-1} in transmittance mode (% T).

The amount of CO_3^{2-} content present in the produced powders was calculated from the percent weight of carbon examined by CHN analysis (Perkin-Elmer series 2, 2400 CHNS/O). Field emission scanning electron microscopy (Zeiss Supra 55VP FESEM) was used to evaluate the morphologies of as-synthesised CHA powders. EDX was then used to roughly identify the ratio of calcium to phosphate of the produced powders.

3. RESULTS AND DISCUSSION

The XRD pattern of as-synthesised CHA powder with different CO_3^{2-}/PO_4^{3-} ratios are shown in Figure 1. Based on the diffraction peaks, all the as-synthesised CHA powders exhibited a single HA (ICDD file no. #09-0432) phase without any formation of secondary phases such as calcium carbonate ($CaCO_3$) and/or calcium oxide (CaO) found.[8] Eight typical peaks of HA were detected within the range $20° \leq (2\,\theta) \leq 70°$, e.g. at $2\,\theta = 26°$, corresponded to (002), three overlapping peaks at $2\,\theta = 32°$ to 34° which represents (211), (300) and (202), $2\,\theta = 40°$ indexed to (310), $2\,\theta = 47°$ to 53° indexed to (222), (213) and (004), respectively.[16] It is noticed that the incorporation of CO_3^{2-} into apatite structure had slightly altered the crystal lattice resulting in the contraction of *a*-axis and extension of *c*-axis relative to the standard reference of pure HA (a = 9.418 Å, c = 6.884 Å), indicating the formation of B-type CHA for all CHA produced powders.[17,18]

By comparing the XRD pattern of as-synthesised CHA powders produced, it was observed that the peaks slightly shifted to lower angle ($2\,\theta$), particularly between $25° < (2\,\theta) < 35°$ with increasing of CO_3^{2-} addition during synthesis. These peaks shift strongly relates to alteration in the crystal lattice because of CO_3^{2-} substitution into the HA crystal structure. Among the produced powders, CHA 4:1 also showed a decrease in the crystallinity, as observed by the broadening of the pattern. This is believed due to the high amount of CO_3^{2-} substituted into the apatite structure. A similar observation was previously reported in our work published elsewhere.[19]

Regardless of the CO_3^{2-}/PO_4^{3-} ratios investigated, the amount of CO_3^{2-} substituted in the produced powders falls in a range of CO_3^{2-} found in human native bone (2 wt % to 10 wt %). The trend of CO_3^{2-} detected (as shown in Table 1) supports the XRD analysis discussed earlier.

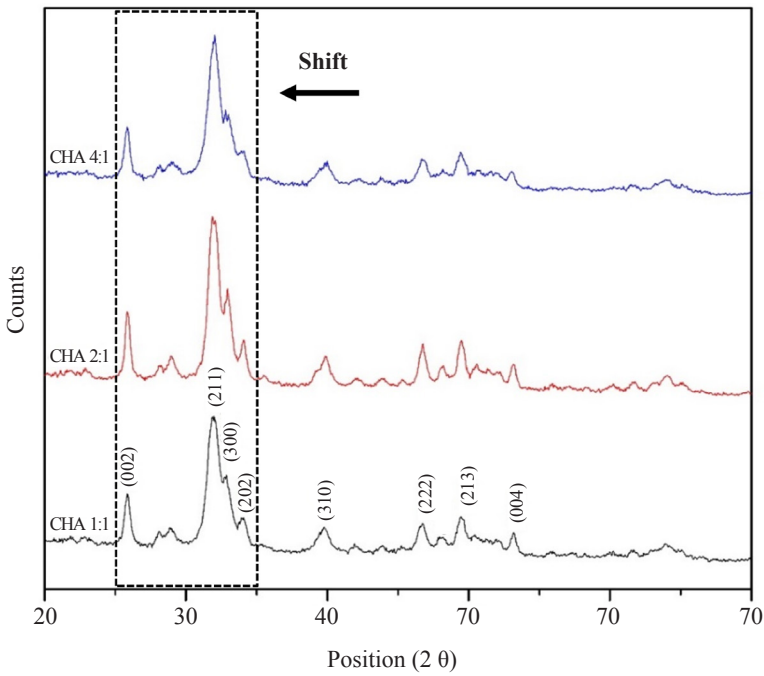

Figure 1: XRD patterns of as-synthesised CHA powder by varying CO_3^{2-}/PO_4^{3-} ratios.

Table 1: Lattice parameter, *c*/*a* ratio and CO_3^{2-} content of as-synthesised CHA powders.

Sample	A = *b*(Å)[b]	*c*(Å)[b]	*c*/*a* ratio	Amount of CO_3^{2-} (wt %)
HA (#09-0432)	9.418	6.884	0.731	–
CHA 1:1	9.432	6.886	0.730	4.200
CHA 2:1	9.413	6.886	0.732	4.860
CHA 4:1	9.410	6.906	0.734	9.250

The FTIR spectra of as-synthesised CHA powders with different CO_3^{2-}/PO_4^{3-} ratios are shown in Figure 2. Based on the spectrum, it is confirmed that all the produced powders remained as B-type CHA, represented by the typical band B-type CO_3^{2-} detected at 870 cm^{-1} to 875 cm^{-1}, 1,410 cm^{-1} to 1,430 cm^{-1} and 1,450 cm^{-1} to 1,470 cm^{-1}.[20,21] The typical bands of A-type CHA, which normally occur at 877 cm^{-1} to 880 cm^{-1}, 1,500 cm^{-1} and 1,540 cm^{-1} to 1,545 cm^{-1} were not found.[10,22] This result is in acceptable agreement with reported literature indicating that B-type CHA (CO_3^{2-} replacing PO_4^{3-}) can be prepared by precipitation reaction in a liquid solution, while A-type CHA (CO_3^{2-} replacing hydroxyl) formed by high temperature reaction of HA with a dry carbon dioxide (CO_2) atmosphere.[23,24]

Interestingly, it is also noticed that the intensity of CO_3^{2-} bands increased proportionally with increasing CO_3^{2-}/PO_4^{3-} ratios, which is consistent with the previous results demonstrated in XRD and CHN analyses. Additionally, the bands were detected at about 473.10 cm^{-1}, 565.74 cm^{-1}, 602.92 cm^{-1}, 983.9 cm^{-1} and 1,032.92 cm^{-1} are attributed to the characteristics bands of the PO_4^{3-} groups. The broad bands in the regions of about 3,300 cm^{-1} to 3,600 cm^{-1} and 1,600 cm^{-1} to 1,700 cm^{-1} show the existence of the hydroxyl groups (OH^-), illustrating the absorbed and occluded water, respectively.[25]

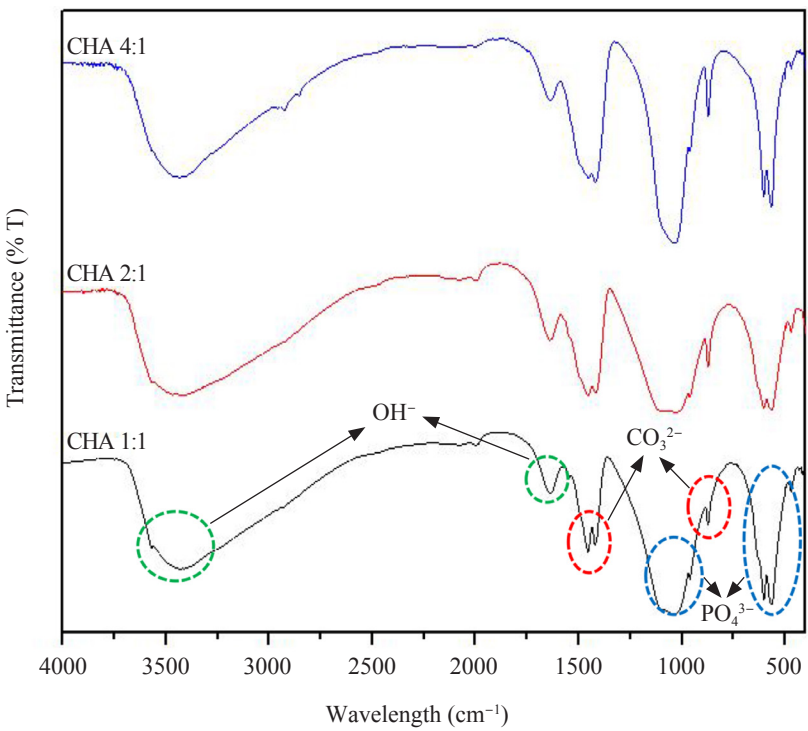

Figure 2: FTIR spectra of as-synthesised CHA powder with variant CO_3^{2-}/PO_4^{3-} ratios.

The morphologies of as-synthesised CHA powders are shown in Figure 3. It is observed similar morphologies of agglomerated nanoparticles for all produced powders. This phenomenon is probably due to the Van der Waals force of attraction between the fine nanoparticles.[13] The finer the particles, the higher the surface energy; therefore, the higher the tendency of the particles to be attracted to each other, resulting in a high degree of agglomeration. As a result, it is difficult to determine the actual size of the individual particles using FESEM.

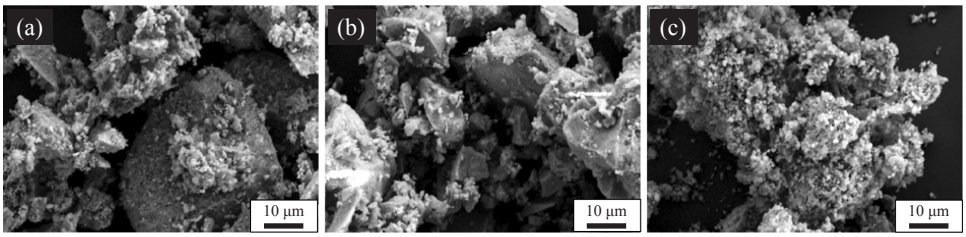

Figure 3: FESEM micrograph of the as-synthesised CHA powders (a) CHA 1:1, (b) CHA 2:1 and (c) CHA 4:1 at magnification of 1.00 K×.

EDX analysis was then carried out to confirm the existence of Ca, phosphorus (P), carbon (C) and oxygen (O) in the as-CHA powder synthesised with different CO_3^{2-}/PO_4^{3-} ratios (as shown in Table 2). The incorporation of CO_3^{2-} into the crystal structure had affected the Ca/P ratio, where the ratio is found relatively higher (> 1.67) than the standard stoichiometric HA for all produced powders.[26] It is also observed that the amount of phosphorus reduced accordingly with the increasing amount of CO_3^{2-}/PO_4^{3-} ratios. This is due to the replacement of PO_4^{3-} groups by CO_3^{2-} ions into the apatite structure. Thus, it can be concluded that the introduction of a higher amount of CO_3^{2-} during synthesis attributed to the higher percentage of CO_3^{2-} substituted into the lattice structure.

Table 2: EDX analysis of as-synthesised CHA powders with different CO_3^{2-}/PO_4^{3-} ratios.

Elements (wt %)	Samples		
	CHA 1:1	CHA 2:1	CHA 4:1
Calcium (Ca)	27.32	23.44	26.20
Phosphorus (P)	14.14	13.51	11.38
Carbon (C)	4.74	6.72	6.90
Oxygen (O)	53.79	56.34	55.52
Ca/P ratio	1.93	1.74	2.30

4. CONCLUSION

B-type CHA powder with different CO_3^{2-}/PO_4^{3-} ratios have been successfully synthesised using direct pouring nanoemulsion method at ambient temperature. The incorporation of higher CO_3^{2-}/PO_4^{3-} ratio into the apatite structure resulted in reduced crystallinity of the powder and concentration of PO_4^{3-}, indicating a higher amount of CO_3^{2-} had successfully substituted into the structure.

5. ACKNOWLEDGEMENTS

Authors sincerely acknowledge the financial support provided by Ministry of Higher Education Malaysia for the Fundamental Research Grant Scheme (FRGS): 203/PBAHAN/6071380.

6. REFERENCES

1. González Ocampo, J. I., Escobar Sierra, D. M. & Ossa Orozco, C. P. (2016). Porous bodies of hydroxyapatite produced by a combination of the gel-casting and polymer sponge methods. *J. Adv. Res.*, 7(2), 297–304, https://doi.org/10.1016/j.jare.2015.06.006.
2. Bang, L. T., Long, B. D. & Othman, R. (2014). Carbonate hydroxyapatite and silicon-substituted carbonate hydroxyapatite: Synthesis, mechanical properties, and solubility evaluations. *Sci. World J.*, 2014, 969876, https://doi.org/10.1155/2014/969876.
3. Uysal, I., Severcan, F., Tezcaner, A. & Evis, Z. (2014). Co-doping of hydroxyapatite with zinc and fluoride improves mechanical and biological properties of hydroxyapatite. *Prog. Nat. Sci. Mater. Int.*, 24(4), 340–349, https://doi.org/10.1016/j.pnsc.2014.06.004.
4. Thian, E. S., Konishi, T., Kawanobe, Y., Lim, P. N., Choong, C., Ho, B., & Aizawa, M. (2013). Zinc-substituted hydroxyapatite: A biomaterial with enhanced bioactivity and antibacterial properties. *J. Mater Sci. Mater. Med.*, 24(2), 437–445, https://doi.org/10.1007/s10856-012-4817-x.
5. Šupová, M. (2015). Substituted hydroxyapatites for biomedical applications: A review. *Ceram. Int.*, 41(8), 9203–9231, https://doi.org/10.1016/j.ceramint.2015.03.316.
6. Yanny Marliana B. I., Wimpenny, I., Bretcanu, O., Dalgarno, K. and El Haj, A. J. (2017). Development of multisubstituted hydroxyapatite nanopowders as biomedical materials for bone tissue engineering applications. *J. Biomed. Mater. Res. A*, 105(6), 1775–1785, https://doi.org/10.1002/jbm.a.36038.
7. Kovaleva, E. S., Shabanov, M. P., Putlayev, V. I., Filippov, Y. Y., Tretyakov, Y. D., & Ivanov, V. K. (2008). Carbonated hydroxyapatite nanopowders for preparation of bioresorbable materials. *Materwiss. Werksttech.*, 39(11), 822–829, https://doi.org/10.1002/mawe.200800383.
8. Othman, R., Mustafa, Z., Loon, C. & Ahmad-Fauzi, M.N. (2016). Effect of calcium precursors and pH on the precipitation of carbonated hydroxyapatite. *Procedia Chem.*, 19, 539–545, https://doi.org/10.1016/j.proche.2016.03.050.

9. Filippov, Y. Y., Klimashina, E. S., Ankudinov, A. B. & Putlayev, V. I. (2011). Carbonate substituted hydroxyapatite (CHA) powder consolidated at 450°C. *J. Phys. Conf. Ser.*, 291, 012036, https://doi.org/10.1088/1742-6596/291/1/012036.
10. Landi, E., Celotti, G., Logroscino, G. & Tampieri, A. (2003). Carbonated hydroxyapatite as bone substitute. *J. Eur. Ceram. Soc.*, 23(15), 2931–2937, https://doi.org/10.1016/S0955-2219(03)00304-2.
11. Kee, C. C., Ismail, H. & Ahmad-Fauzi, M.N. (2013). Effect of synthesis technique and carbonate content on the crystallinity and morphology of carbonated hydroxyapatite. *J. Mater. Sci. Technol.*, 29(8), 761–764, https://doi.org/10.1016/j.jmst.2013.05.016.
12. Rey, C., Combes, C., Drouet1, C. & Glimcher, M. (2010). Bone mineral: Update on chemical composition and structure. *Osteoporos. Int.*, 20, 1013–1021, https://doi.org/10.1007%2Fs00198-009-0860-y.
13. Mohammad, N. F., Othman, R., Abdullah, N. A. & Yeoh, F. Y. (2016). In vitro evaluation of mesoporous carbonated hydroxyapatite in MC3T3-E1 osteoblast cells. *Procedia Chem.*, 19, 259–266, https://doi.org/10.1016/j.proche.2016.03.103.
14. Ezekiel, I., Shah Rizal, K., Yanny Marliana, B. I. & Ahmad-Fauzi, M. N. (2018). Nanoemulsion synthesis of carbonated hydroxyapatite nanopowders: Effect of variant CO_3^{2-}/PO_4^{3-} molar ratios on phase, morphology and bioactivity. *Ceram. Int.*, 44(11), 13082–13089, https://doi.org/10.1016/j.ceramint.2018.04.128.
15. Germaini, M. M., Detsch, R., Grünewald, A., Magnaudeix, A., Lalloue, F., Boccaccini, A. R. & Champion, E. (2017). Osteoblast and osteoclast responses to A/B type carbonate-substituted hydroxyapatite ceramics for bone regeneration. *Biomedical Materials*, 12(3), 035008, https://doi.org/10.1088/1748-605x/aa69c3.
16. Safarzadeh, M., Ramesh, S., Tan, C. Y., Chandran, H., Ching, Y. C., Ahmad-Fauzi, M.N. & Teng, W. D. (2019). Sintering behaviour of carbonated hydroxyapatite prepared at different carbonate and phosphate ratios. *Bol. Soc. Esp. Cerám. V.*, Forthcoming.
17. Kovaleva, E. S., Shabanov, M. P., Putlyaev, V. I., Tretyakov, Y. D., Ivanov, V. K., & Silkin, N. I. (2009). Bioresorbable carbonated hydroxyapatite $Ca_{10-x}Na_x(PO_4)_{6-x}(CO_3)_x(OH)_2$ powders for bioactive materials preparation. *Cent. Eur. J. Chem.*, 7(2), 168–174, https://doi.org/10.2478/s11532-009-0018-y.
18. Ivanova, T. I., Frank-Kamenetskaya, O. V., Kol'tsov, A. B. & Ugolkov, V. L. (2001). Crystal structure of calcium-deficient carbonated hydroxyapatite. thermal decomposition. *J. Solid State Chem.*, 160(2), 340–349, https://doi.org/10.1006/jssc.2000.9238.

19. Muhammad Syazwan, M. N. & Yanny Marliana, B. I. (2019). The influence of simultaneous divalent cations (Mg^{2+}, Co^{2+} and Sr^{2+}) substitution on the physico-chemical properties of carbonated hydroxyapatite. *Ceram. Inter.*, 45(12), 14783–14788, https://doi.org/10.1016/j.ceramint.2019.04.208.
20. Kumar, G. S., Thamizhavel, A., Yokogawa, Y., Kalkura, S. N. & Girija, E. K. (2012). Synthesis, characterization and in vitro studies of zinc and carbonate co-substituted nano-hydroxyapatite for biomedical applications. *Mater. Chem. Phys.*, 134(2–3), 1127–1135, https://doi.org/10.1016/j.matchemphys.2012.04.005.
21. Zhou, W. Y., Wang, M., Cheung, W. L., Guo, B. C. & Jia, D. M. (2008). Synthesis of carbonated hydroxyapatite nanospheres through nanoemulsion. *J. Mater. Sci. Mater. Med.*, 19, 103–110, https://doi.org/10.1007/s10856-007-3156-9.
22. Wong, W. Y. & Ahmad-Fauzi M.N. (2016). Synthesis and sintering-wet carbonation of nano-sized carbonated hydroxyapatite. *Procedia Chem.*, 19, 98–105, https://doi.org/10.1016/j.proche.2016.03.121.
23. Wu, Y. S., Lee, Y. H. & Chang, H. C. (2009). Preparation and characteristics of nanosized carbonated apatite by urea addition with coprecipitation method. *Mater. Sci. Eng. C*, 29(1), 237–241, https://doi.org/10.1016/j.msec.2008.06.018.
24. Lafon, J. P., Champion, E. & Bernache-assollant, D. (2008). Processing of AB-type carbonated hydroxyapatite $Ca_{10-x}(PO_4)_{6-x}(CO_3)_x(OH)_{2-x-2y}(CO_3)_y$ ceramics with controlled composition. *J. Eur. Ceram. Soc.*, 28(1), 139–147, https://doi.org/10.1016/j.jeurceramsoc.2007.06.009.
25. Yanny Marliana, B. I. & Ahmad-Fauzi, M. N. (2011). Effect of a novel approach of sintering on physical properties of carbonated hydroxyapatite. *J. Mater. Sci. Eng. B*, 1, 157–163.
26. Sprio, S., Tampieri, A., Landi, E., Sandri, M., Martorana, S., Celotti, G. & Logroscino, G. (2008). Physico-chemical properties and solubility behaviour of multi-substituted hydroxyapatite powders containing silicon. *Mater. Sci. Eng. C*, 28(1), 179–187, https://doi.org/10.1016/j.msec.2006.11.009.